Observation of a Saturation in the Time Scale for Multifragment Emission in Symmetric Heavy-Ion Collisions

E. Bauge,[1],[6] A. Elmaani,[1] Roy A. Lacey,[1] J. Lauret,[1] N. N. Ajitanand,[1] D. Craig,[2] M. Cronqvist,[2] E. Gualtieri,[2] S. Hannuschke,[2] T. Li,[2] B. Llope,[2] T. Reposeur,[2] A. Vander Molen,[2] G. D. Westfall,[2] J. S. Winfield,[2] J. Yee,[2] S. Yennello,[2] A. Nadasen,[3] R. S. Tickle,[4] and E. Norbeck[5]

[1] *Department of Chemistry, State University of New York at Stony Brook, Stony Brook, New York 11794-3400*

[2] *National Superconducting Cyclotron Laboratory and Department of Physics, Michigan State University, East Lansing, Michigan 48824-1321*

[3] *Department of Physics, University of Michigan at Dearborn, Dearborn, Michigan 48128*

[4] *Department of Physics, University of Michigan, Ann Arbor, Michigan 48109-1120*

[5] *Department of Physics, University of Iowa, Iowa City, Iowa 52242*

[6] *Institut des Science Nucléaires de Grenoble, 53 Avenue des Martyrs, 38026 Grenoble Cedex, France*

(Received 4 January 1993)

We have measured two-fragment reduced-velocity correlation functions of the intermediate mass fragments (IMF: $3 \leq Z \leq 7$) produced in multifragment final states for the Kr + Nb system (E/A = 35, 45, 55, 65, and 75 MeV). From the measured correlation functions we extract mean IMF emission lifetimes (τ) which are observed to decrease from $\tau \approx 400$ fm/c at $E/A = 35$ MeV to $\tau \approx 125$ fm/c at $E/A = 55$ MeV. For beam energies in excess of $E/A = 55$ MeV, no further decrease in τ is observed, indicating a possible saturation of the mean emission lifetime for IMF produced in multifragment exit channels.

PACS numbers: 25.70.Pq

A major objective of current intermediate energy heavy-ion research is to probe the properties of nuclear matter at "high" energy density. Nuclear fragmentation leading to multifragment final states—with one or more intermediate mass fragment (IMF: $3 \geq Z \geq 20$)—is predicted to be the major decay mode for nuclear systems produced at high density and temperature [1,2]. Recognizing the potential utility of multifragment final states as probes for hot compressed nuclear matter, many researchers have devoted substantial efforts to the study of the dominant mechanisms responsible for nuclear fragmentation (see for example [3–12]).

Experimental information pertaining to the time scale for multifragment emission may very well provide important clues about the space-time characteristics of fragmentation processes. Similarly, such experimental information can provide important constraints which allow a distinction between the different models which predict multifragment final states [13–15]. Currently, there is great interest in the distinction between simultaneous multifragment final states and those produced via a binary disintegration sequence.

Results from many dynamical model calculations predict short emission lifetimes ($\tau \approx 100$ fm/c) for simultaneous multifragment final states [15–20]. In contrast, only a limited set of experiments has focused on the time scale for multifragment final states involving IMF [6,21–23]. Emission lifetimes determined from these studies (for different systems and beam energies) range from $\tau \geq 500$ fm/c down to $\tau \approx 100$ fm/c.

A study of the evolution of the emission time scale (for multifragment final states) over a broad range of incident energies is, without doubt, an important prerequisite for an understanding of the space-time characteristics of nuclear fragmentation processes.

In this Letter we exploit the reduced-velocity correlation technique [24] to characterize the mean emission lifetime for multifragment final states produced in central collisions of Kr + Nb (E/A = 35, 45, 55, 65, and 75 MeV). We present experimental evidence which shows that the mean emission lifetime for Z = 3–7 fragments exhibits an initial decrease from $\tau \approx 400$ fm/c at $E/A = 35$ MeV to $\tau \approx 125$ fm/c at $E/A = 55$ MeV. However, no further decrease in τ is observed as the beam energy is increased from $E/A = 55$ MeV to $E/A = 75$ MeV. We interpret this result as evidence for a saturation in the mean emission lifetime for IMF produced in multifragment exit channels.

The ^{84}Kr beams (E/A = 35 to 75 MeV) used in the measurements were provided in 10 MeV steps by the K1200 cyclotron at the National Superconducting Cyclotron facility (NSCL). Charged reaction products were detected with the MSU FourPI Array [25]. The MSU FourPI Array consists of a main ball of 170 phoswich counters (arranged in 20 hexagonal and 10 pentagonal subarrays) covering angles from 23° to 157° and a forward array of 45 phoswich counters covering angles from 7° to 18°. Thirty Bragg curve counters are installed in front of the hexagonal and pentagonal subarrays; they were operated in ion chamber mode with a pressure of 100 torr of C_2F_6. The hexagonal anodes of the five most forward Bragg curve counters are segmented, giving a total of 55 separate ΔE gas counters for the measurements.

The Bragg curve counters served as ΔE detectors for charged particles that stopped in the fast plastic scintillator of the main ball. Consequently, the array was

capable of detecting charged fragments from $Z = 1$ to $Z = 12$. Low energy thresholds for the main ball were 17 MeV/nucleon, 3 MeV/nucleon, and 5 MeV/nucleon for fragments of $Z = 1, 3$, and 12, respectively. The low energy threshold for the forward array was $\approx$ 17 MeV/nucleon. The beam intensity was approximately 100 electrical pA of ^{40}Ar, and the thickness of the natural Nb target was 1.0 mg/cm^2. Data were taken with a minimum bias trigger (charged particle multiplicity $m \geq 2$) and a more central trigger ($m \geq 5$).

In our analysis, two-fragment reduced-velocity correlation functions [$V_{\rm red} = V_{\rm rel}/(Z_1+Z_2)^{1/2}$] were constructed from fragments ($3 \leq Z \leq 7$) detected at polar angles ranging from 7° to 35°. $V_{\rm rel}$ is the relative velocity between two detected fragments whose charges are Z_1 and Z_2, respectively.

Following the approach commonly exploited in interferometry studies [26,27], the two-fragment reduced-velocity correlation function $C(V_{\rm red})$ is defined as the ratio of two distributions [24]:

$$C(V_{\rm red}) = \frac{N_{\rm cor}(V_{\rm red})}{N_{\rm uncor}(V_{\rm red})}, \quad (1)$$

where $N_{\rm cor}(V_{\rm red})$ is the observed reduced-velocity distribution for fragment pairs selected from the same event (coincidence distribution) and $N_{\rm uncor}(V_{\rm red})$ is the reduced-velocity distribution for fragment pairs selected from mixed events (background distribution). For the results presented here, mixed events were obtained by randomly selecting each member of a fragment pair from different events with the same impact parameter range. Impact parameters were determined by way of cuts on the total transverse momentum [28,29]. Central collisions corresponding to an average impact parameter $\leq 0.30 b_{\rm max}$ were used for each beam energy in our analysis. $b_{\rm max}$ is the maximum estimated impact parameter.

Experimental two-fragment reduced-velocity correlation functions for IMF emitted in central collisions of Kr + Nb are shown in Fig. 1. Figures 1(a)–1(e) show results for beam energies of E/A = 35, 45, 55, 65, and 75 MeV, respectively. All of the correlation functions (open squares) shown in Fig. 1 exhibit pronounced deficits or anticorrelations for $V_{\rm red}$ values less than 30 units ($10^{-3}c$). These deficits are a manifestation of the repulsive final-state Coulomb interaction between the emitted fragments. A careful examination of Fig. 1 also reveals that the anticorrelations at small $V_{\rm red}$ increase as the bombarding energy is increased from $E/A = 35$ MeV to $E/A = 55$ MeV. A reduction in the space-time extent of an emitting source leads to larger final-state Coulomb interactions and hence, larger anticorrelations at small $V_{\rm red}$ [24,27]. Consequently, we interpret the observed trend of the anticorrelations as supporting evidence for the notion that the space-time extent (of the emitter) decreases as the bombarding energy is increased from $E/A = 35$ MeV to $E/A = 55$ MeV/A.

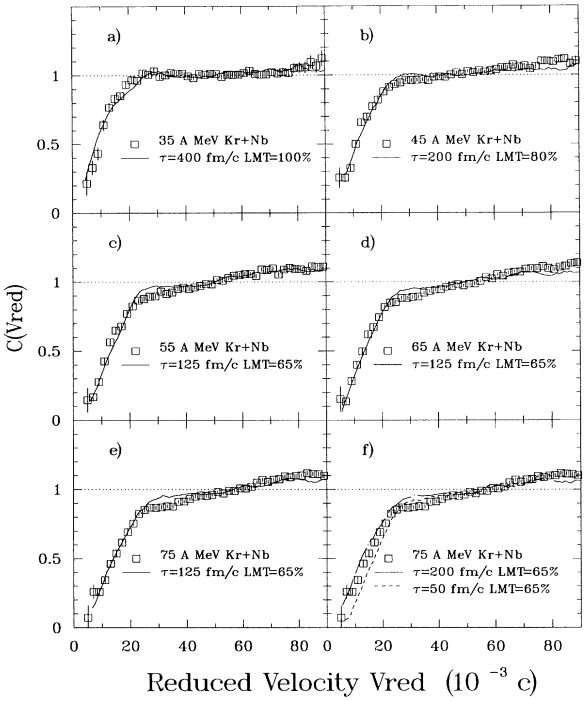

FIG. 1. Correlation functions for Z = 3–7 fragments for $E/A = 35$ MeV (a), $E/A = 45$ MeV (b), $E/A = 55$ MeV (c), $E/A = 65$ MeV (d), $E/A = 75$ MeV (e), $E/A = 75$ MeV (f). The solid, dashed, and dot-dashed curves represent calculated correlation functions for the τ and LMT values shown in the figure.

The curves shown in Fig. 1 represent calculated two-fragment reduced-velocity correlation functions derived from a modified version of the trajectory code MENEKA [30]. This code evaluates the classical three-body Coulomb trajectories of fragments sequentially emitted from the surface of an equilibrated source. The time delays (t) between the emitted fragments is characterized by an exponential probability distribution $P(t) \propto \exp -t/\tau$, where τ is the emission lifetime. The code takes explicit account of recoil effects and the Coulomb influence of the daughter nucleus. In addition, it utilizes the measured fragment energy, angular, and charge distributions, and takes into account the acceptance of the FourPI Array. Two free parameters were utilized in the calculations; τ and the linear momentum transfer (LMT). It is important to recognize, however, that the LMT variable fixes the mass and charge of the emitter. To illustrate this point we note that 65% LMT gives rise to an emitting system whose respective mass and charge is 35% less than that of the combined mass and charge of the target and projectile. For the Kr + Nb system, this leads to an emitter of mass $A = 115$ (65% of the composite mass) and charge $Z = 50$ (65% of the composite charge). We should point out here that the calculated correlation functions show much stronger sensitivity to

LMT at large V_{red} than at small V_{red}. This being the case, the choice of LMT values does not have a significant effect on the determined τ values.

The comparisons between measured and calculated correlation functions shown in Fig. 1 indicates that the experimental correlation functions are consistent with mean emission lifetimes which range from $\tau \approx 400$ fm/c for $E/A = 35$ MeV to $\tau \approx 125$ fm/c for $E/A = 55$ MeV. These results also show that the emission lifetime decreases monotonically as the beam energy is raised from $E/A = 35$ MeV to $E/A = 55$ MeV. Even more striking in this figure is the fact that τ shows no significant change (to lower values) for beam energies greater than $E/A = 55$ MeV. It is tempting to speculate that the latter observation might be related to a saturation of the mean emission lifetime for multifragment exit channels. Such a saturation could result from the onset of simultaneous multifragmentation at $E/A \approx 55$ MeV. If simultaneous multifragment emission becomes the dominant decay mechanism for energies ≥ 55 MeV/nucleon then no significant change in τ is expected as the beam energy is increased. It is noteworthy that the observed τ values for $E/A \geq 55$ MeV are consistent with those ($\tau \approx 100$ fm/c) predicted for multifragment decays which originate from bulk instabilities of nuclear matter at low density [1,2,15,16,18,19].

Figure 1(f) illustrates the sensitivity of the calculations to τ for a fixed LMT. In this figure we compare the experimental correlation function previously shown in Fig. 1(e) (for $E/A = 75$ MeV) to results from calculations employing two different τ values. The open squares in the figure represent the experimental correlation function; the dashed and dot-dashed curves represent calculations for τ values of 50 fm/c and 200 fm/c, respectively. The calculated curve for $\tau = 200$ fm/c overpredicts the data while that for $\tau = 50$ fm/c underpredicts the data. The calculated result for $\tau = 125$ fm/c [Fig. 1(e)] is clearly in better agreement with the data.

The effect of LMT on the calculated correlation function is illustrated in Fig. 2(a) for $E/A = 75$ MeV. In this figure we compare results for 100% LMT (squares) and 50% LMT (circles) for a fixed value of $\tau = 100$ fm/c. The comparison shows little or no difference between the two correlation functions at small V_{red} ($V_{red} \leq 20$). On the contrary, there are comparatively larger differences for V_{red} values ≥ 20. Specifically, it can be seen that the correlation function calculated for 50% LMT shows a distinctly larger slope (for V_{red} values ≥ 30) than that for 100% LMT. The experimental correlation functions displayed in Fig. 1 also show positive slopes for $V_{red} \geq 30$ which are more pronounced for the higher beam energies. These slopes are attributable to dynamical correlations which result from the recoil of the emitter as well as its Coulomb influence.

The correlation functions shown in Fig. 2(a) assume constant LMT values. Since LMT fluctuations can potentially distort the correlation function, we have investigated the effect of these fluctuations. Figure 2(b) compares calculated correlation functions for a fixed LMT value (squares) and a Gaussian LMT distribution (circles). The distribution takes into account fluctuations of both the emitter's mass (M), and charge (Z) ($\sigma_{M,Z} = 0.2\langle M, Z\rangle$) as well as its velocity (v) ($\sigma_v = 0.2\langle v\rangle$). The comparison shows no appreciable difference between the two correlation functions. Hence, we conclude that LMT fluctuations do not lead to significant distortions of the correlation functions.

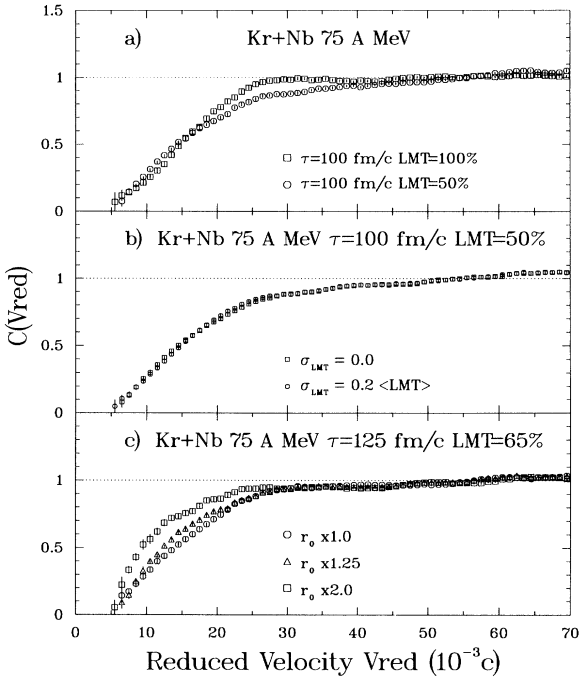

FIG. 2. (a) Calculated correlation functions for 50% LMT (open circles) and 100% LMT (open squares) for $E/A = 75$ MeV and $\tau = 100$ fm/c. (b) Calculated correlation functions for a fixed LMT value (squares) and a Gaussian distribution of LMT values (circles). (c) Calculated correlation functions for three different emitter sizes with fixed LMT and τ. Emitter size is characterized by the variable r_0. Curves are shown for r_0 (circles), $1.25r_0$ (triangles), and $2.0r_0$ (squares).

On the one hand, the dependence of the correlation function on LMT leads us to conclude that the positive slopes displayed by the experimental correlation functions might be due to incomplete momentum transfer. On the other hand, we conclude that the determined τ values are not sensitive to our choice of LMT because τ is constrained primarily by the anticorrelation observed in the correlation functions for V_{red} values ≤ 20. The fact that the experimental correlation function shows a much smaller slope (for $V_{red} \geq 20$) for $E/A = 35$ MeV than that for $E/A \geq 55$ MeV is consistent with the notion that LMT decreases with increasing beam energy. The respective values of LMT employed in our calculations (for each beam energy) are displayed in Fig. 1. It is perhaps possible to have better agreement between

the experimental and calculated correlation functions (at large V_{red} values) by choosing a different set of LMT values. However, such a set would not alter our conclusions pertaining to τ.

The calculated correlation functions shown in Fig. 1 were performed with the assumption that the radius of the emitting system (R) is given by $R = r_0 A^{1/3}$ where $r_0 = 1.44$ fm and A is the mass number of the emitter. If nuclear expansion plays an important role in the production of multifragment final states, such an expansion can lead to emitter sizes which are larger than the ones used in our calculations. In view of this, calculations were also performed for different emitter sizes assuming fixed values for both LMT and τ. For illustrative purposes, we compare the correlation functions obtained for three different r_0 parameters ($E/A = 75$ MeV, $\tau = 125$ fm/c, and LMT = 65%) in Fig. 2(c). In this figure, the open circles, triangles, and squares represent the correlation function obtained for r_0, $1.25r_0$, and $2r_0$, respectively. In contrast to the results for different LMT (discussed above), the comparison shows that the shape of the correlation function—for $V_{red} < 20$—is sensitive to big changes in the emitter size; namely, the strength of the anticorrelation at small V_{red} is reduced as the size of the emitter is increased. Our calculations show that a relatively small increase ($\leq 30\%$) in the emitter size can be compensated for by a reduction in τ. Consequently, if nuclear expansion is important for the production of multifragment final states involving IMF, then the observed saturation of τ would represent a saturation in the space-time extent of the emitting source.

The mean emission lifetimes obtained from the experimental data are summarized in Fig. 3. Here, we have plotted τ as a function of beam energy; the error bars shown in the figure reflect the sensitivity of the calculations to τ. The τ value (≈ 400 fm/c) obtained for $E/A = 35$ MeV is somewhat larger than a previous value extracted for an asymmetric system at the same beam energy [23]. Figure 3 shows that the mean emission lifetime decreases from $\tau \approx 400$ fm/c at $E/A = 35$ MeV to $\tau \approx 125$ fm/c at $E/A = 55$ MeV. For beam energies greater than $E/A = 55$ MeV, τ assumes a constant value ≈ 125 fm/c, indicating a saturation of the mean lifetime for IMF emission in multifragment final states.

In summary, we have measured two-fragment reduced-velocity correlation functions for the symmetric Kr + Nb system over a broad range of bombarding energies. These correlation functions indicate mean fragment emission lifetimes which initially decrease with increasing beam energy. However, for beam energies greater than $E/A = 55$ MeV, τ is observed to saturate at ≈ 125 fm/c. This emission lifetime is consistent with those predicted for multifragment disintegration resulting from bulk instabilities of nuclear matter at low density. The fact that τ does not show any significant change for beam energies greater than $E/A = 55$ MeV leads us to speculate that the onset of simultaneous multifragmentation in the Kr + Nb system may be occurring at a beam energy ≈ 55 MeV/nucleon.

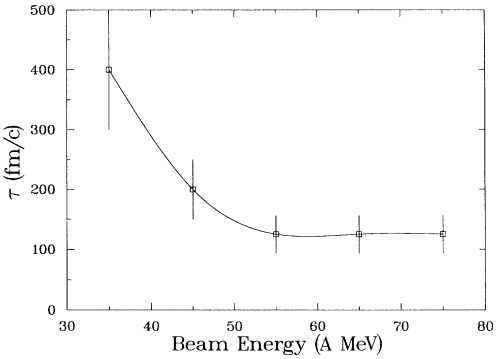

FIG. 3. Mean emitter lifetime as a function of beam energy. The solid curve is drawn to guide the eye.

This work was supported in part by the National Science Foundation under Grants No. PHY-89-13815 (NSCL) and No. PHY-92-11611 (Stony Brook).

[1] G. Bertsch *et al.*, Phys. Lett. **126B**, 9 (1983).
[2] D. H. E. Gross, Rep. Prog. Phys. **53**, 605 (1990).
[3] *Proceedings of the Symposium on Nuclear Dynamics and Nuclear Disassembly* (World Scientific, Singapore, 1989).
[4] R. T. de Souza *et al.*, Phys. Lett. B **268**, 6 (1991).
[5] D. R. Bowman *et al.*, NSCL Report No. MSUCL-850, July 1992 (unpublished).
[6] D. Cebra *et al.*, Phys. Rev. Lett. **64**, 2246 (1990).
[7] J. Hubele *et al.*, Z. Phys. A **340**, 263 (1991).
[8] Y. Blumenfeld *et al.*, Phys. Rev. Lett. **66**, 576 (1991).
[9] C. A. Ogilvie *et al.*, Phys. Rev. Lett. **67**, 1214 (1991).
[10] V. E. Viola *et al.*, Nucl. Phys. **A538**, 291c (1992).
[11] G. Bizard *et al.*, Phys. Lett. B **276**, 413 (1992).
[12] T. Ethvignot *et al.*, Phys. Rev. C **46**, 637 (1992).
[13] J. Randrup *et al.*, Nucl. Phys. **A356**, 223 (1981).
[14] W. A. Friedman, Phys. Rev. Lett. **60**, 2125 (1988).
[15] W. Bauer *et al.*, Phys. Rev. Lett. **61**, 1888 (1992).
[16] D. H. Boal *et al.*, Phys. Rev. C **37**, 91 (1988).
[17] G. Peilert *et al.*, Phys. Rev. C **29**, 1402 (1989).
[18] J. Aichelin *et al.*, Phys. Rev. C **37**, 2451 (1988).
[19] E. Suraud, Nucl. Phys. **A495**, 73 (1989).
[20] P. Danielewicz *et al.*, Nucl. Phys. **A533**, 712 (1991).
[21] R. Trockel *et al.*, Phys. Rev. Lett. **59**, 2844 (1987).
[22] R. Bougault *et al.*, Phys. Lett. B **232**, 291 (1989).
[23] Y. D. Kim *et al.*, Phys Rev. Lett. **67**, 14 (1991).
[24] Y. D. Kim *et al.*, Phys. Rev. C **45**, 338 (1992).
[25] G. D. Westfall *et al.*, Nucl. Instrum. Methods Phys. Res., Sect. A **238**, 347 (1985).
[26] D. H. Boal *et al.*, Rev. Mod. Phys. **62**, 553 (1990).
[27] A. Elmaani *et al.*, Phys. Rev. C **43**, R2474 (1991).
[28] T. Li *et al.*, MSU report (to be published).
[29] H. G. Ritter *et al.*, Nucl. Phys. **A488**, 651c (1988).
[30] A. Elmaani *et al.*, Nucl. Instrum. Methods Phys. Res., Sect. A **313**, 401 (1992).